CEPC NOTE

CEPC-RECO-2018-002

April 1, 2018

Higgs Signal Reconstruction at CEPC-v4 Baseline Detector for the CEPC CDR

CEPC Simulation Group

Abstract

Using the CEPC software chain, the reconstruction performance of the Higgs boson signals at CEPC-v4 baseline detector are studied. In this note, the distributions of the reconstructed invariant mass of the Higgs boson at the $\nu\nu$H, H→ bb, cc, gg, $\mu\mu$, $\gamma\gamma$, ZZ* and WW* events are shown. This set of reconstruction performance can be used as the basic benchmark for detector and algorithm optimization.

E-mail address: zhaohang@ihep.ac.cn

Contents

1 Introduction **2**

2 Detector Geometry and Reconstruction Tool **2**

3 Reconstruction Results **2**
3.1 Higgs→ $\mu\mu$ 2
3.2 Higgs→ $\gamma\gamma$ 2
3.3 Higgs→ bb, cc and gg 3
3.4 Higgs→ ZZ* 5
3.5 Higgs→ WW* 5

4 Summary **7**

1 Introduction

The historic discovery of the Higgs boson in 2012 by the ATLAS and CMS collaborations at the Large Hadron Collider (LHC) has opened a new era in particle physics [1][2]. Proposed by the Chinese high energy physics community, the CEPC [3] project will take advantage of the clean environment of e^+e^- collisions to increase the precision of Higgs boson properties and Electroweak measurements. As for now, the CEPC project is at the stage of Conceptual Design Report (CDR) study. A full software chain of simulation and reconstruction has been developed for the studies of the detector design and the physics performance analysis. This note is devoting to the physics performance studies of the Higgs boson signals at A PFA Oriented Detector for HIggS factory (APODIS), CEPC-v4 detector geometry, which is also the baseline detector geometry for the CEPC CDR studies. These reconstruction results can offer a set of performance benchmarks for detector optimization and physics analysis algorithm study.

This note is organized as follows. Section 2 gives a brief introduction to the detector geometry and reconstruction tools. Section 3 shows the reconstruction results of the Higgs boson signals using the simulated samples of Higgs $\rightarrow$ bb, cc, gg, WW*, ZZ*, $\gamma\gamma$ and $\mu\mu$. The summary is given in Section 4.

2 Detector Geometry and Reconstruction Tool

The CEPC software group has developed two main conceptual benchmark detector geometries till now, CEPC_v1 for the Pre-CDR studies and CEPC_v4 for the CDR studies. The detail description of the detectors can be found in CEPC Note CEPC-SIMU-2017-001 [4]. In this manuscript, the CEPC_v4 geometry is used.

The default reconstruction algorithm of the CEPC software chain is based on the Arbor [5], a particle flow algorithm developed for the CEPC study. The parameters of Arobr have been adjusted according to the CEPC-v4 geometry in the version ArborforV4, which can be found at the CEPC software website [6]. The collision energy is set to be 250 GeV in this manuscript, and all the samples can be also accessed at the website.

3 Reconstruction Results

At CEPC, more than 20% of the Higgs bosons are generated with a pair of neutrinos (from ZH, Z $\rightarrow \nu\nu$ events, the W fusion events and their interference). In these events, besides a few ISR photons, all the visible final state particles are generated from the Higgs decay, providing clean, and inclusive samples for the detector response study of the Higgs signals. In this section, the invariant mass distributions of $\nu\nu$H events are presented, with Higgs bosons decay into different final states. Each distribution is normalized to unit area and the sample statistic is indicated in the corresponding figure captions.

3.1 Higgs$\rightarrow \mu\mu$

The Higgs boson decay to $\mu\mu$ is a rare process with a branching ratio of 0.022% for a Higgs boson mass of 125 GeV. This measurement provides a performance benchmark for the tracking system design. The reconstructed Higgs boson invariant mass of selected Higgs$\rightarrow \mu\mu$ is shown in Fig 1. The long tail in the left side is caused by the unsuccessful reconstruction of the muon.

3.2 Higgs$\rightarrow \gamma\gamma$

The SM Higgs boson has 0.2% the chance to decay into a pair of photons. Since photons could be easily identified from other particles, this channel becomes one of the discovery channel for the Higgs boson at

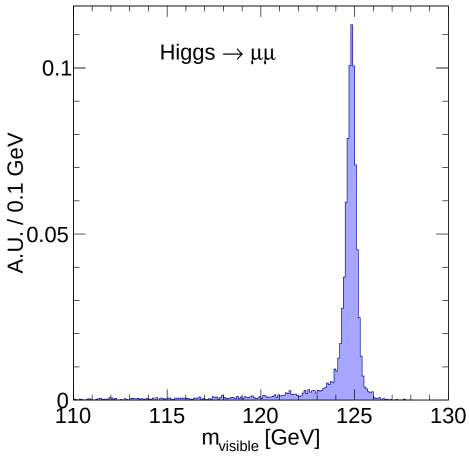

Figure 1: The reconstructed Higgs invariant mass of $H \to \mu\mu$ events at the CEPC v_4 detector geometry.

the LHC. At the CEPC, this channel also serves as a benchmark to characterize the ECAL performance. The performance required in photon reconstruction and energy resolution is a challenge for the electromagnetic calorimeter (ECAL) design. Using the reconstructed $\upsilon\upsilon H, H \to \gamma\gamma$ sample and calculate the invariant mass of two most energetic photon candidates, we acquire the objective distributions see Fig. 2. This measurement provides a performance benchmark for the ECAL design and photon reconstruction.

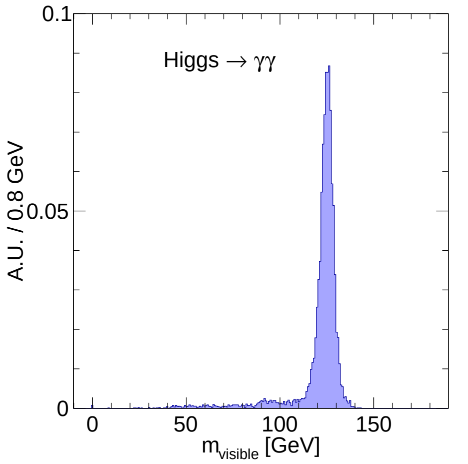

Figure 2: The reconstructed Higgs invariant mass of $H \to \gamma\gamma$ events at the CEPC v_4 detector geometry.

3.3 Higgs→ bb, cc and gg

The majority of the SM Higgs boson decay into di-jet final states: 58%/3% into a pair of b/c quarks via the direct Yukawa coupling, and 8% into a pair of gluon mainly via top quark loop. Unlike the LHC, these di-jet events could be easily identified simply using its invariant masses. In this section, the distributions of $\upsilon\upsilon H, H \to bb, cc, gg$ with or without cleaning will be shown.

The inclusive distributions shown in Fig. 3 clearly exhibit non gaussian, asymmetric patterns. These patterns are induced from visible ISR photons, neutrinos generated in Higgs decay cascade, and the detector acceptance. Applying the corresponding cuts in the standard cleaning procedure, these patterns disappears, see Fig. 4.

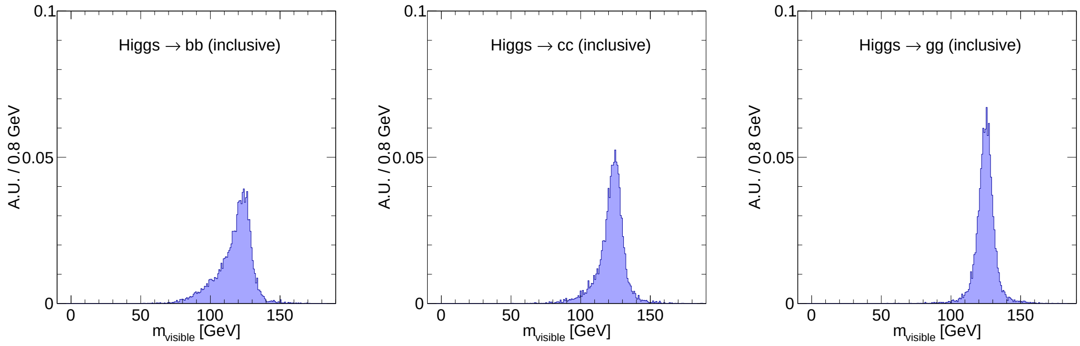

Figure 3: Total visible mass distribution of $\nu\nu H, H \to di-jet$ events, without cleanning

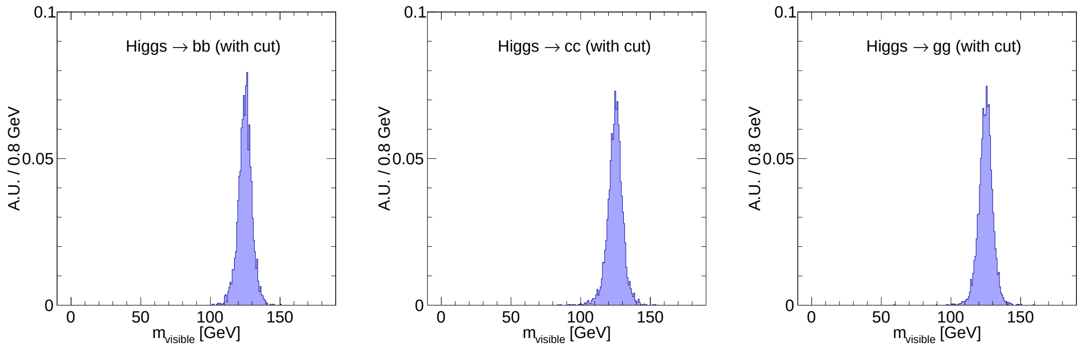

Figure 4: Total visible mass distribution of $H \to di-jet$ events, with cleanning

-	$H \to bb$	$H \to cc$	$H \to gg$
Sample statistic	10k	10k	9.6k
$\epsilon_{ISRveto}$	94%	94%	94%
$\epsilon_{neutrinoveto}$	41%	69%	94%
$\epsilon_{acceptance}$	74%	74%	74%
σ_m/m	3.60 ± 0.07%	3.76 ± 0.05%	3.69 ± 0.04%

Table 1: Statistics, cut efficiencies on the $\nu\nu H, H \to dijet$ samples and the relative mass resolution after the cleaning.

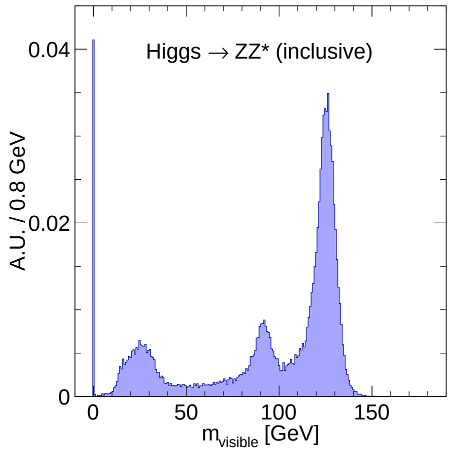

Figure 5: Total visible mass distribution of $H \to ZZ^*$ events

The corresponding efficiencies and statistics are summarized in Table 1. For three different decay modes, the neutrino veto condition has different efficiencies, and vetoed more than half of the $H \to bb$ events. The other two condition have essentially identical efficiencies. After the cleaning, the relative mass resolution for three different decay modes converges to a similar level.

3.4 Higgs→ ZZ*

Roughly 3% of the SM Higgs boson decays into a pair of Z boson: limited by the Higgs mass, one of the Z boson is on shell and the other off shell. The cascade decay of $H \to ZZ^* \to 4l$ is the other Higgs discovery channel at the LHC, as the leptons are clean signature. At the CEPC, combing the $Br(H \to ZZ^*)$ measurements and the g_{HZZ} measurements via the recoil mass methods leads to a direct, model independent determination of Higgs total width, therefore is of strong physics interests.

The Z boson decays into all kinds of SM fermions except the top quark. Thus, a successful reconstruction of the $Br(H \to ZZ^*)$ signal requires a proper reconstruction of leptons, taus, missing energy and jets. After vetoing the events with energetic, visible ISR photons, the total visible mass distribution of $Br(H \to ZZ^*)$ events at APODIS is shown in Fig. 5. Several peaks could be easily identified at this distribution. The peak at zero corresponding to the total invisible decay mode where both Z and Z* decays into neutrinos and has a branching ratio of roughly 4%. The peak at the Higgs boson mass (125 GeV) is corresponding to the total visible mode. The other two peaks are corresponding to the conjugation case where $Z \to visible, Z^* \to invisible$ and $Z^* \to visible, Z \to visible$. Because of the heavy flavor and τ component of the Z boson decay, the peak at 125 GeV and at the Z boson mass exhibit a tail at the low mass side.

3.5 Higgs→ WW*

The decay mode of $H \to WW^*$ has the second largest decay branching ratio (21.5%) for the SM Higgs. The invariant mass distribution of the inclusive $H \to WW^*$ events is shown in Fig. 6. About 28% of the $H \to WW^*$ events cascades to $\mu\nu qq$ or $e\nu qq$ final states. In the $\nu\nu H$ events, those semi-leptonic decay events have very clear signature: significant missing energy/momentum, one isolated lepton and two jets. Fig. 7 shows the visible mass of all the reconstructed particle except the prong lepton generated in W boson decay. A clear peak at the W mass and A bump corresponding to the off-shell W* could clearly be identified in this distribution.

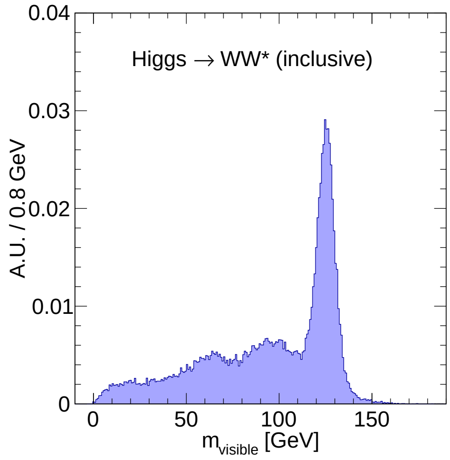

Figure 6: Total visible mass distribution of $H \to WW^{*}$ events

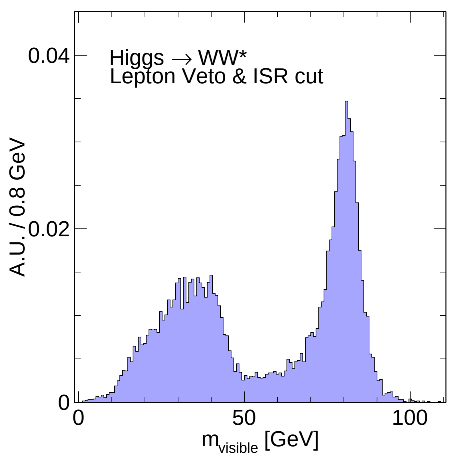

Figure 7: Visible mass distribution with all the final states except the prong lepton of $H \to WW^{*} \to l\nu qq$ events

4 Summary

To conclude, the CEPC baseline design (APODIS + Arbor) achieves a successful reconstruction of all the physics objects (lepton, photon, tau, jet and missing energy/momentum) for the Higgs measurement. In all the major decay modes of the SM Higgs boson, the Higgs signal is well established. The reconstruction of the Higgs boson invariant mass with Higgs bosons decay to different final states provides a set of performance benchmarks for the detector and physics analysis algorithm optimization.

References

[1] ATLAS Collaboration, Observation of a new particle in the search for the Standard Model Higgs Boson with the ATLAS detector at the LHC, Phys. Lett. B716 (2012) 1-29, ArXiv: 1207.7214

[2] CMS Collaboration, Observation of a new boson at a mass of 125 GeV with the CMS experiment at the LHC, Phys. Lett. B716 (2012) 30-61, ArXiv: 1207.7235

[3] The CEPC-SPPC Study Group, CEPC-SPPC Preliminary Conceptual Design Report, http://cepc.ihep.ac.cn/preCDR/main_preCDR.pdf

[4] CEPC Software Group, Full Simulation Software at CEPC, http://cepcdoc.ihep.ac.cn/DocDB/0001/000167/001/cepc-sim.pdf

[5] M. Ruan and H. Videau, Arbor, *a new approach of the Particle Flow Algorithm*, arxiv:1403.4784 [physics.ins-det]

[6] CEPC Software Website, http://cepcsoft.ihep.ac.cn/